Mathematically Modelling the Cellular Effects of Alcohol Consumption during Photobiomodulation Light Therapy

Alicia Mathew (20820160) & Yuliana Zelisko (20943221)

AMATH/BIOL 382 – Winter 2024

Brian Ingalls

University of Waterloo

Abstract

Photobiomodulation (PBM) is a form of light therapy that employs specific wavelengths of light in the red to near-infrared spectrum to stimulate cells and tissues. This non-invasive therapy targets chromophores within cells, particularly in mitochondria, triggering responses that enhance ATP production and influence cellular activity. PBM is widely applied in wound healing, cell regeneration, promoting anti-inflammatory responses, and pain relief.

Cellular molecules do not respond to PBM in isolation but through complex feedback mechanisms consisting of numerous signaling molecules and pathways. These dynamic responses change significantly over time depending on different environmental conditions, making it a challenge to track and predict accurately. Building on previous studies, Hsieh et al. (2022) developed a mathematical model using ordinary differential equations to describe PBM's impact on mitochondrial cytochrome c oxidase, an enzyme vital for ATP synthesis. This report broadens the model's scope to assess the potential inhibitory effects of common concerns like alcohol consumption on the mechanisms underlying PBM treatment efficacy, specifically the processes that regulate oxidative stress during stimulation. The simulated results show that mild, moderate, and severe alcohol consumption all lead to a prolonged period of unregulated oxidative stress within the mitochondria during PBM stimulation, which could lead to harmful effects.

Table of Contents

1. Introduction

1.1 Overview of PBM Therapy

Photobiomodulation (PBM) therapy, which operates within the red to near-infrared (NIR) wavelength spectrum of 630-1200 nm, is recognized for its ability to stimulate biological processes in tissues, as outlined by Hamblin & Demidova (2006), without inflicting thermal damage (Chung et al., 2011). This range is optimally selected for its capacity to penetrate deep tissue and promote cellular metabolism and rejuvenation. The core mechanism of PBM is its interaction with cytochrome c oxidase (COX), an essential enzyme within the mitochondrial respiratory chain that has absorption peaks within this wavelength range. (Wong-Riley et al., 2005) The light targets COX to displace inhibitory nitric oxide (NO), thereby boosting cellular respiration and energy production, as seen in increased ATP synthesis, which in turn supports cell growth, migration, and survival under stress (Hamblin & Demidova, 2006).

PBM's efficacy extends beyond the cellular level, with numerous animal model studies demonstrating positive outcomes across a range of conditions. Supported by a substantial number of clinical trials, the majority of which are randomized controlled trials, PBM shows promising results in relieving pain (Fulop et al., 2010; Konstantinovic et al., 2010), reducing inflammation (Xavier et al., 2010), and accelerating wound healing (Whelan et al., 2001; Peplow et al., 2010; Lucas et al., 2002). This breadth of evidence reinforces the utility of PBM in clinical practice.

Moreover, PBM distinguishes itself from other light therapies that may use potentially harmful ultraviolet (UV) light or ionizing radiation, by employing non-ionizing light sources. (Lampl et al., 2007) This reduces the risk of DNA damage and the potential for carcinogenic effects, enhancing the safety profile of PBM and rendering it an appropriate option for repeated use, especially in managing chronic conditions.

1.2 Cellular Responses to PBM

PBM exerts its biological effects primarily through the action of chromophores, which are light-sensitive molecules present within cells. These molecules, particularly mitochondrial COX, have a high affinity for specific wavelengths of light. When exposed to red light (600–810 nm) or near-infrared light (810–1064 nm), chromophores like COX absorb these photons, leading to the displacement of nitric oxide (NO) that is bound to COX. (Karu et al., 2005) This displacement is not merely a physical process but one that activates the enzyme, setting off a cascade of biological responses. The activation of COX by light enhances the mitochondrial electron transport chain's (ETC) efficiency, increasing the production of ATP. (Pastore et al., 1996) The proton gradient across the mitochondrial membrane is the driving force behind ATP synthesis, an integral part of cellular regeneration. (Amaroli et al., 2021)

An integral part of this biological cascade includes the production of reactive oxygen species (ROS), such as superoxide, O_2^-. These ROS are by-products of normal mitochondrial metabolism but are markedly increased following PBM-induced ETC activity, modulating signaling pathways. (Hamblin & Demidova, 2006) While excessive ROS can lead to oxidative stress and cellular damage, the controlled production generated by PBM can promote adaptive and regulatory responses. Superoxide, in particular, can be transformed to hydrogen peroxide, which then participates in downstream signaling cascades, enhancing cell survival and function. (Wong et al., 2017) Thus, the role of ROS is crucial for signaling cellular adaptation and serves as a potential indicator in fine-tuning PBM parameters for achieving desired therapeutic outcomes.

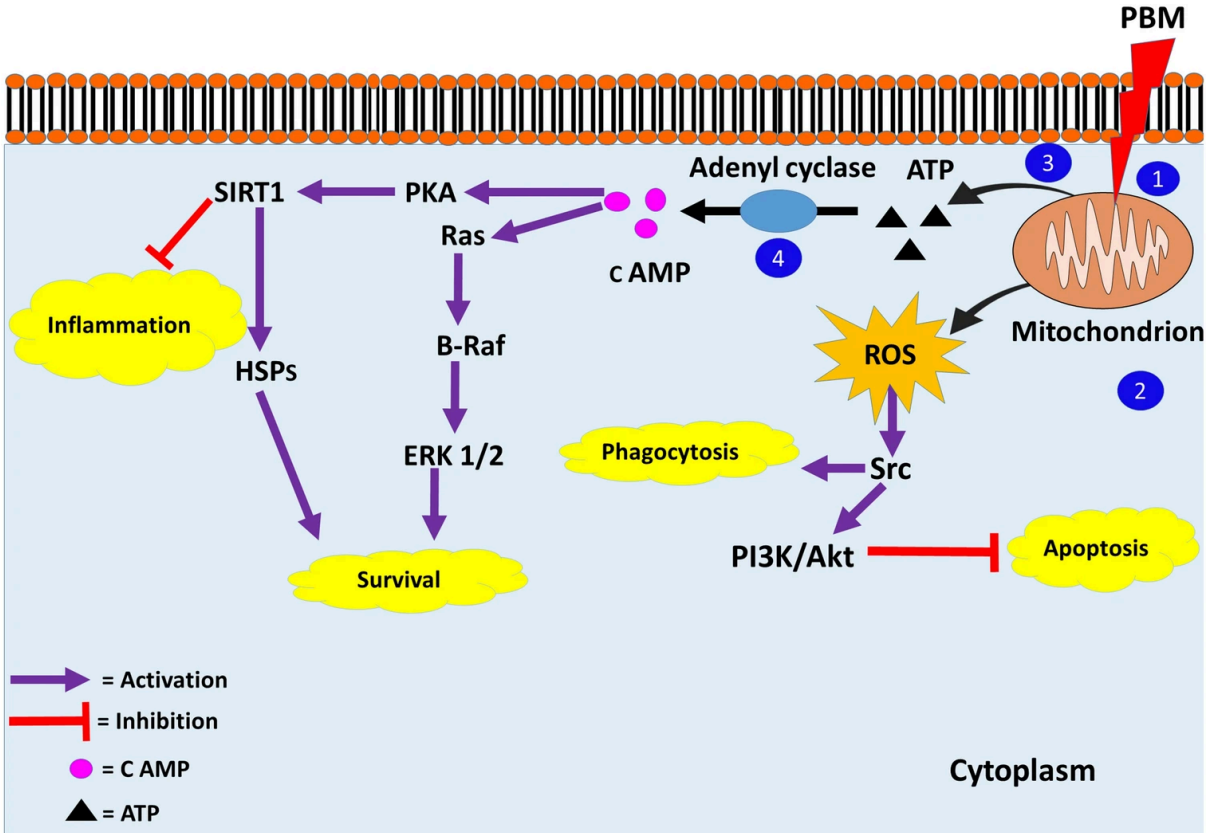

Figure 1 – **PBM's effect through ROS**. 1) Mitochondrial COX absorbs light 2) ROS is produced, activating processes that promote phagocytosis and inhibit apoptosis 3) ATP production increases, activating key pathways which further inhibit inflammation and promote cell survival (Bathini et al., 2020)

1.3 Clinical Applications and the Significance of PBM

PBM has gained recognition for its diverse clinical applications and its effectiveness in treating a spectrum of conditions, rapidly repairing tissues, reducing inflammation, and offering neuroprotection. PBM is applied across diverse medical fields, from dental pain relief (Sfondrini et al., 2020) to treating musculoskeletal disorders (Gendron & Hamblin, 2019) and enhancing cognitive abilities. (Salehpour et al., 2018) However, optimizing PBM parameters such as dosage, wavelength, fluence, and power densities remains a significant challenge, with ongoing research aimed at tailoring these factors to specific therapeutic outcomes.

These parameters are influenced by the target area (e.g. the brain, muscles, or joints) as well as by biological factors like skin melanin content, which can affect light penetration depth and require personalized treatment protocols. The exploration of these parameters is critical in establishing standard protocols that can enhance the consistency and predictability of PBM outcomes as well as maximize the therapeutic potential of PBM across different clinical settings.

1.4 Impact of External Factors on PBM Efficacy

The efficacy of PBM extends beyond clinical settings and is significantly affected by external factors such as environmental conditions and personal lifestyle choices. In particular, chronic alcohol consumption has been linked to impaired mitochondrial function, potentially impairing the mechanisms PBM aims to enhance by altering membranal signal transduction pathways and increasing oxidative stress (Jung et al., 2010). This is highly relevant given PBM's dependence on mitochondrial activity for its therapeutic effects. Understanding these external influences is essential for customizing PBM protocols to individual patients, particularly in clinical research where controlling such variables is crucial for accurately evaluating therapeutic outcomes.

2. Mathematical Model

2.1 Motivation for the Model

The mathematical model developed by Hsieh et al. (2022) is fundamentally rooted in the experimental work of Amaroli et al. (2021), which investigated the effects of PBM on mitochondrial activity and ROS production. Amaroli et al. conducted their research using an *in vitro* setup, allowing for precise control over environmental conditions and direct observation of mitochondrial responses without the complexities and variables inherent in live animal models. This was crucial for isolating the effects of specific laser wavelengths and power settings on mitochondrial complexes.

The study specifically utilized isolated bovine liver mitochondria, exposing them to varying fluences of 980 nm laser light. This controlled environment facilitated the accurate measurement of key mitochondrial functions, including ATP production, oxygen consumption, and the generation of ROS. The setup also ensured that the data collected directly reflected the impact of PBM on mitochondria, minimizing external biological influences that could obscure results.

2.2 Structure and Objective of the Model

Building upon the findings from Amaroli et al., Hsieh et al. developed a model that uses ODEs to describe the dynamic behavior of mitochondrial processes in reaction to PBM, aiming to replicate the dose-dependent effects observed under laboratory conditions in the Amaroli et al. experiments. Their key objective was to provide a predictive tool that can simulate the biological

effects of different PBM parameters (e.g. wavelength, power density) on mitochondrial activity. (Hsieh et al., 2022) This modeling approach allows for the exploration of optimal PBM settings for therapeutic purposes, aiming to maximize beneficial outcomes while minimizing harmful effects such as excessive ROS production.

The model's accuracy was tested by comparing its output with the experimental results of Amaroli et al., ensuring that it effectively captures the essence of mitochondrial responses to PBM. This validation process was crucial for confirming the model's utility in predicting clinical efficacy and guiding treatment protocols. By integrating experimental data into a robust mathematical model, Hsieh et al. aim to advance the precision of PBM therapies in clinical settings, enhancing both their efficacy and safety.

2.3 Model Description and Parameters

The Hsieh et al. model (Figure 2) outlines the complex intramitochondrial interactions that occur during PBM. At the center, it includes COX, signifying its central role in the model. The parameters and their respective processes in the model are further broken down as follows:

1. **Light Interaction with COX**: The model begins with light stimulation (L), leading to the photodissociation of inhibitory NO from COX, characterized by the rate constant k_{LNO}, enhancing mitochondrial respiration. Also included is the rate of the reaction light-induced superoxide production (k_{LO2}).
2. **NO and Oxygen Dynamics**: The model includes parameters for NO binding to COX (k_{NOon}) and oxygen binding to COX (k_{O2app}), essential for ATP production.
3. **COX Activation States**: COX is modeled in different states—free, bound to NO, or bound to oxygen—reflecting its functional status under varying PBM conditions.
4. **Superoxide (O_2^-) and ROS Dynamics**: The rate constant (k_{O2-}) for the reduction of cytochrome c, consuming superoxide, is highlighted due to its impact during PBM.
5. **Cytochrome C Redox Cycling**: The model factors in the redox states of cytochrome c (cyt c^{3+}/cyt c^{2+}), the rate of cytochrome c reduction (k_{III}), as well as the rate of oxygen consumption by oxidized COX (k_{IV}) to emphasize these roles in electron transport and ROS balance.
6. **Metabolism of NO**: The conversion of NO into nitrate (k_{NO3-}) and nitrite (k_{NO2-}) is represented, linking NO metabolism to the model's framework.
7. **Production and Consumption of NO**: Lastly, the model accounts for NO production from precursors (k_{NOpro}) and its consumption within cellular processes (k_{NOcom}), pivotal for mitochondrial regulation.

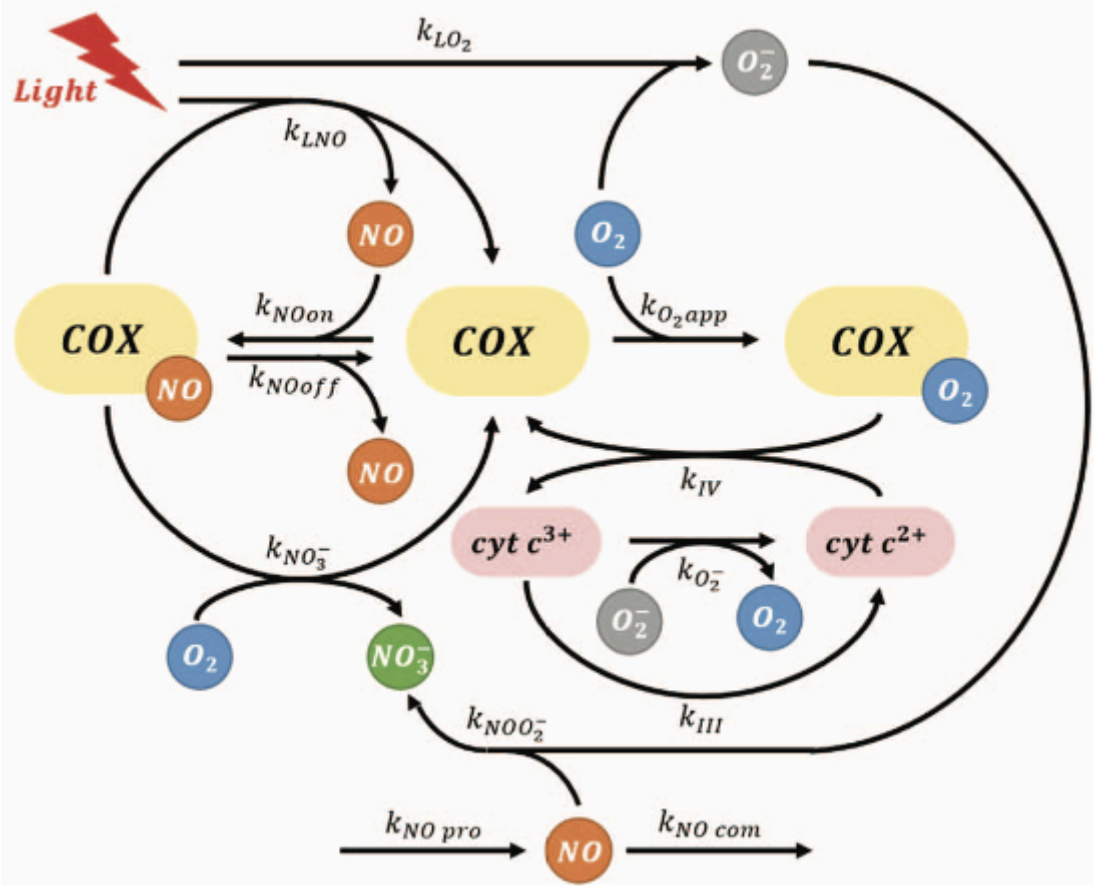

Figure 2 – **Hsieh et al. Intramitochondrial Model of PBM Mechanisms** (Hsieh et al., 2020)

Each parameter represents a biological process that contributes to the PBM mechanism. Some of these parameters (Table 1) were extrapolated directly from simulating the experiments outlined in the Amaroli et al. paper while others were taken from prior PBM studies. The complexity of the Hsieh et al. model mirrors the multifaceted nature of mitochondrial responses to PBM and their original focus was to simulate the effect of different energy densities of light on the dynamics of COX, COX-NO, O_2, NO, and O_{2-}.

TABLE 1 – PARAMETERS AND INITIAL CONDITIONS (Hsieh et al., 2022)

Parameter	Value	Source
k_{LNO}	10 a.u.$^{-1}$ s^{-1}	Fitted using ATP synthesis data from Amaroli et al., 2021
k_{LO2}	0.25 a.u.$^{-1}$ s^{-1}	
k_{De}	4.75	
k_{NOon}	40 $\mu M^{-1}s^{-1}$	Antunes et al., 2004
k_{NOoff}	0.01 s^{-1}	
k_{O2app}	140 $\mu M^{-1}s^{-1}$	
k_{III} (state 3)	23.3 s^{-1}	
k_{IV}	1.5 $\mu M^{-1}s^{-1}$	

k_{NO3-}	0.0423 $\mu M^{-1}s^{-1}$	Estimated from Aguirre et al., 2010 parameters
k_{O2-}	0.26 $\mu M^{-1}s^{-1}$	Markevich & Hoek., 2015
k_{NOO2-}	7000 $\mu M^{-1}s^{-1}$	Pryor & Squadrito, 1995
k_{NOpro}	20.41 μMs^{-1}	Esimated from Giulivi et al., 1998 experimental data
k_{NOcom}	75 s^{-1}	Estimated for steady state concentration ~0.25 μM
Initial Condition	**Value**	**Source**
[L]	0.1 a.u. per J/cm^2	Fitted using ATP synthesis data from Amaroli et al., 2021
$[O_2]$	150 μM	Antunes et al., 2004
$[COX]_{tot}$	140 μM	
$[cyt\ c]_{tot}$	200 μM	
[NO]	0 μM	Steady state
$[O_{2-}]$	0 μM	Steady state

Table 1 shows parameter values for k_{LNO} and k_{LO2} using units of "arbitrary units inverse" per second (a.u.$^{-1}$ s^{-1}), which refers to a normalized unit of measure used to quantify the concentrations that are not directly tied to a standard concentration measurement like molarity. This allows for the comparison of results across different experimental setups. For instance, a rate constant of 10 a.u.$^{-1}s^{-1}$ for k_{LNO} implies that the photodissociation of inhibitory NO from COX proceeds at a rate that would deplete 10 arbitrary units per second if no other processes were occurring. Similarly, an initial condition of 0.1 a.u. per J/cm^2 for [L] suggests that for each Joule of energy delivered per square centimeter, the light intensity contributing to the reaction is 0.1 in the chosen arbitrary units of the model. Thus, to investigate the effect of a fluence of 7.7 J/cm^2, the model would accept an [L] value of 0.77 based on this conversion.

2.4 Model Breakdown and Simplification

The core of the Hsieh et al. model is a series of ODEs that quantify the time-dependent behavior of these molecular species involved in the PBM response. These equations include:

$$\frac{d[COX-NO]}{dt} = k_{NOon}[NO][COX] - k_{NOoff}[COX-NO] - k_{LNO}[L][COX-NO] - k_{NO_3^-}[O_2][COX-NO]$$

$$\frac{d[COX]}{dt} = -k_{NOon}[NO][COX] + k_{NOoff}[COX-NO] + k_{LNO}[L][COX-NO] + k_{NO_3^-}[O_2][COX-NO] + k_{IV}[\text{cyt } c^{2+}][COX-O_2] - k_{O_2app}[O_2][COX]$$

$$\frac{d[COX-O_2]}{dt} = -k_{IV}[\text{cyt } c^{2+}][COX-O_2] + k_{O_2app}[O_2][COX]$$

$$
\begin{aligned}
\frac{d[\text{cyt c}^{2+}]}{dt} &= -k_{IV}[\text{cyt c}^{2+}][COX - O_2] - \left(k_{III} + k_{O_2^-}[O_2^-]\right)[\text{cyt c}^{2+}] + \left(k_{III} + k_{O_2^-}[O_2^-]\right)[\text{cyt c}]_{tot} \\
\frac{d[\text{cyt c}^{3+}]}{dt} &= k_{IV}[\text{cyt c}^{2+}][COX - O_2] - k_{III}[\text{cyt c}^{3+}] - k_{O_2^-}[O_2^-][\text{cyt c}^{3+}] \\
\frac{d[O_2]}{dt} &= -k_{O_2 app}[O_2][COX] - k_{LO_2}[L][O_2] - k_{NO_3^-}[O_2][COX - NO] + k_{O_2^-}[O_2^-][\text{cyt c}^{3+}] \\
\frac{d[NO]}{dt} &= -k_{NOon}[NO][COX] + k_{NOoff}[COX - NO] + k_{LNO}[L][COX - NO] + k_{NOpro} \\
&\quad - k_{NOcom}[NO] - k_{NOO_2^-}[NO][O_2^-] \\
\frac{d[L]}{dt} &= -k_{LNO}[L][COX - NO] - k_{LO_2}[L][O_2] \\
\frac{d[O_2^-]}{dt} &= k_{LO_2}[L][O_2] - k_{O_2^-}[O_2^-][\text{cyt c}^{3+}] - k_{NOO_2^-}[NO][O_2^-]
\end{aligned}
$$

Conservation laws are also incorporated into the model to ensure the accuracy and reliability of the simulation. These laws represent the total amount of the following species, which remains constant over time, as it merely changes form but is neither created nor destroyed within the system. For COX, the total concentration, $[\text{COX}]_{\text{tot}}$, is the sum of all forms of COX: its free state, bound to NO, and bound to O_2. Similarly, for cytochrome c (cyt c), the total concentration, $[\text{cyt c}]_{\text{tot}}$, is the sum of its oxidized (cyt c^{3+}) and reduced (cyt c^{2+}) forms:

$$
\begin{aligned}
[COX]_{tot} &= [COX] + [COX - NO] + [COX - O_2] \\
[\text{cyt c}]_{tot} &= [\text{cyt c}^{3+}] + [\text{cyt c}^{2+}]
\end{aligned}
$$

Using these conservations, Hsieh et al. applied a quasi-steady state approximation to COX and cytochrome c, to express the three states of COX as follows:

$$
\begin{aligned}
[COX] &= \frac{[COX]_{tot}}{\left(1 + b + \frac{c}{d + k_{IV}\left(\frac{-B + \sqrt{B^2 - 4AC}}{2A}\right)}\right)} \\
[COX - NO] &= b[COX] \\
[COX - O_2] &= \frac{c}{d - k_{O_2 app} k_{IV}[O_2][COX]}[COX]
\end{aligned}
$$

$$
\begin{aligned}
b &= \frac{k_{NOon}[NO]}{k_{NOoff} + k_{LNO}[L] + k_{NO_3^-}[O_2]} \\
c &= k_{O_2 app}\left(k_{III} + k_{O_2^-}[O_2^-]\right)[O_2] \\
d &= k_{IV}\left(k_{III} + k_{O_2^-}[O_2^-]\right)[\text{cyt c}]_{tot} \\
e &= -k_{O_2 app}[O_2][\text{cyt c}]_{tot} \\
A &= k_{IV} + bk_{IV} \\
B &= bd + d + c - ek_{IV} \\
C &= -ed
\end{aligned}
$$

This allowed for the overall simplification of the model, particularly for the ODEs of oxygen, nitric oxide, light, and superoxide whose dynamics can be simulated using the total concentrations of COX and cytochrome c rather thanthe biased initial conditions of their various different states. (Hsieh et al., 2022) Therefore, using these constants, the final, simplified model used for simulations is:

$$\frac{d[\text{cyt c}^{2+}]}{dt} = -k_{IV}[\text{cyt c}^{2+}][COX - O_2] - \Big(k_{III} + k_{O_2^-}[O_2^-]\Big)[\text{cyt c}^{2+}] + \Big(k_{III} + k_{O_2^-}[O_2^-]\Big)[\text{cyt c}]_{tot}$$

$$\frac{d[\text{cyt c}^{3+}]}{dt} = k_{IV}[\text{cyt c}^{2+}][COX - O_2] - k_{III}[\text{cyt c}^{3+}] - k_{O_2^-}[O_2^-][\text{cyt c}^{3+}]$$

$$\frac{d[O_2]}{dt} = \frac{-B + \sqrt{B^2 - 4AC}}{2A} - k_{LO_2}[L][O_2] - \frac{bk_{NO_3^-}[O_2][COX]_{tot}}{\left(1 + b + \frac{c}{d + k_{IV}\left(\frac{-B+\sqrt{B^2-4AC}}{2A}\right)}\right)} + \frac{ck_{IV}k_{O_2^-}[O_2^-][COX]_{tot}[\text{cyt c}]_{tot}}{ck_{IV}[COX]_{tot} + \Big(k_{III} + k_{O_2^-}[O_2^-]\Big)\Big((1+b)\Big(d + k_{IV}\Big(\frac{-B+\sqrt{B^2-4AC}}{2A}\Big)\Big) + c\Big)}$$

$$\frac{d[NO]}{dt} = \frac{\Big(-k_{NOon}[NO] + b\Big(k_{NOoff} + k_{LNO}[L]\Big)\Big)[COX]_{tot}}{\left(\frac{-B+\sqrt{B^2-4AC}}{2A}\right)} + k_{NOpro} - k_{NOcom}[NO] - k_{NOO_2^-}[NO][O_2^-]$$

$$\frac{d[L]}{dt} = k_{De}\left(-\frac{bk_{LNO}[L][COX]_{tot}}{\left(1 + b + \frac{c}{d + k_{IV}\left(\frac{-B+\sqrt{B^2-4AC}}{2A}\right)}\right)} - k_{LO_2}[L][O_2]\right)$$

$$\frac{d[O_2^-]}{dt} = k_{LO_2}[L][O_2] - \frac{ck_{IV}k_{O_2^-}[O_2^-][COX]_{tot}[\text{cyt c}]_{tot}}{ck_{IV}[COX]_{tot} + \Big(k_{III} + k_{O_2^-}[O_2^-]\Big)\Big((1+b)\Big(d + k_{IV}\Big(\frac{-B+\sqrt{B^2-4AC}}{2A}\Big)\Big) + c\Big)} - k_{NOO_2^-}[NO][O_2^-]$$

3. Model Extension

3.1 Alcohol's Impact on Mitochondrial Dynamics

Understanding how alcohol functions as well as its effects on PBM is important due to its prevalent use in society. Alcohol, particularly ethanol, the primary form of alcohol in beverages, can significantly impact cellular processes and mitochondrial behavior, leading to detrimental effects on health. People categorized as at-risk alcohol users, defined by the National Institute on Alcohol Abuse and Alcoholism (NIAAA) as women consuming more than 3 drinks on any single day or more than 7 drinks per week, and men consuming more than 4 drinks on any single day or more than 14 drinks per week, face heightened risks. (NIAAA, 2023) Analyzing the effects of ethanol on at-risk alcohol users can give us a better understanding of the chemical interactions that occur and ensure that patients are safe when seeking PBM treatment.

Studies have indicated that ethanol can alter mitochondrial structure, impacting vital organs such as the heart and liver. (Hoek et al., 2002; Roberts et al., 1994) The presence of ethanol modifies ATP levels and boosts the production of ROS, including superoxide. In the context of PBM therapy, which promotes the reduction of cytochrome c^{3+} to cytochrome c^{2+}, a process that consumes superoxide and produces O_2, the excessive production of superoxide caused by ethanol can interfere with this reduction. This can result in a delayed decrease in superoxide levels and a higher peak in its concentration during PBM, potentially complicating treatment outcomes for individuals with chronic alcohol exposure.

This extension examines ethanol transformation to acetaldehyde within mitochondria, focusing on how this metabolite contributes to cellular stress. Ethanol, once ingested, is metabolized into acetaldehyde, a compound that significantly impacts mitochondrial function. (Manzo-Avalos & Saavedra-Molina, 2010) In the extended model, mitochondrial acetaldehyde concentrations are quantified using different levels of alcohol consumption: mild, moderate, and severe. This conversion is crucial for understanding how alcohol intake translates into varying degrees of mitochondrial stress and potential damage. (Eriksson et al., 2003)

3.2 Sensitivity Analysis of Alcohol Level on Superoxide Concentration

To better understand the effect of different levels of alcohol consumption, a sensitivity analysis was performed using perterbations of mitochondrial acetaldehyde concentrations. (Eriksson et al., 2003) A baseline acetaldehyde concentration of 0 μM represents the case where there is no alcohol presence in the blood during PBM, whereas Table 2 shows the concentrations used to simulate the three categories of alcohol intake. In addition, the rate constant k_{AOH} was also introduced to represent the rate at which alcohol reacts to form O_2^- with respect to the blood alcohol concentration, denoted as [Acetaldehyde], in the new model.

TABLE 2 – ACETALDEHYDE PARAMETERS AND INITIAL CONDITIONS

Parameter	Value		Source
k_{AOH}	0.95 $\mu M^{-1}s^{-1}$		Muggli et al., 1998
[Acetaldehyde]	Mild	1.25 μM	Eriksson et al., 2003
	Moderate	3.28 μM	
	Severe	26.16 μM	

The value of 0.95 $\mu M^{-1}s^{-1}$ for k_{AOH} was chosen based on existing literature regarding acetaldehyde dynamics and serves as an approximate reference point rather than an accurate representation. All other parameter values in the extended model remained the same as in Table 1. To incorporate this, the only modification to the original model was made to the differential equation for O_2^-, where an additional term was added to represent the additional surge in superoxide production caused by increased levels of acetaldehyde, as shown in the equation below.

$$\frac{d[O_2^-]}{dt} = k_{LO_2}[L][O_2] - \frac{ck_{IV}k_{O_2^-}[O_2^-][COX]_{tot}[\text{cyt c}]_{tot}}{ck_{IV}[COX]_{tot} + \left(k_{III} + k_{O_2^-}[O_2^-]\right)\left((1+b)\left(d + k_{IV}\left(\frac{-B+\sqrt{B^2-4AC}}{2A}\right)\right)+c\right)} - k_{NOO_2^-}[NO][O_2^-] + \left(k_{AOH}[\text{Acetaldehyde}][O_2^-]\right)$$

An additional important parameter included in the model is the fluence, or energy density, of light used i.e. the amount of energy (Joules) that is being irradiated per unit area (cm^2). The original experiments performed by Amaroli et al. focus a light of 980 nm wavelength at 15

difference fluences ranging from 7.7 J/cm^2 to 107.8 J/cm^2. In this extension, to demonstrate the alcohol-induced effects during PBM therapy, a subset of these values were chosen, namely 38.5, 61.6, 84.7, and 107.8 J/cm^2, and the time-dependent behavior of superoxide was simulated using the varying concentrations of acetaldehyde for mild, moderate, and severe alcohol intake.

3.3 Results and Discussion of Effects on PBM Efficacy

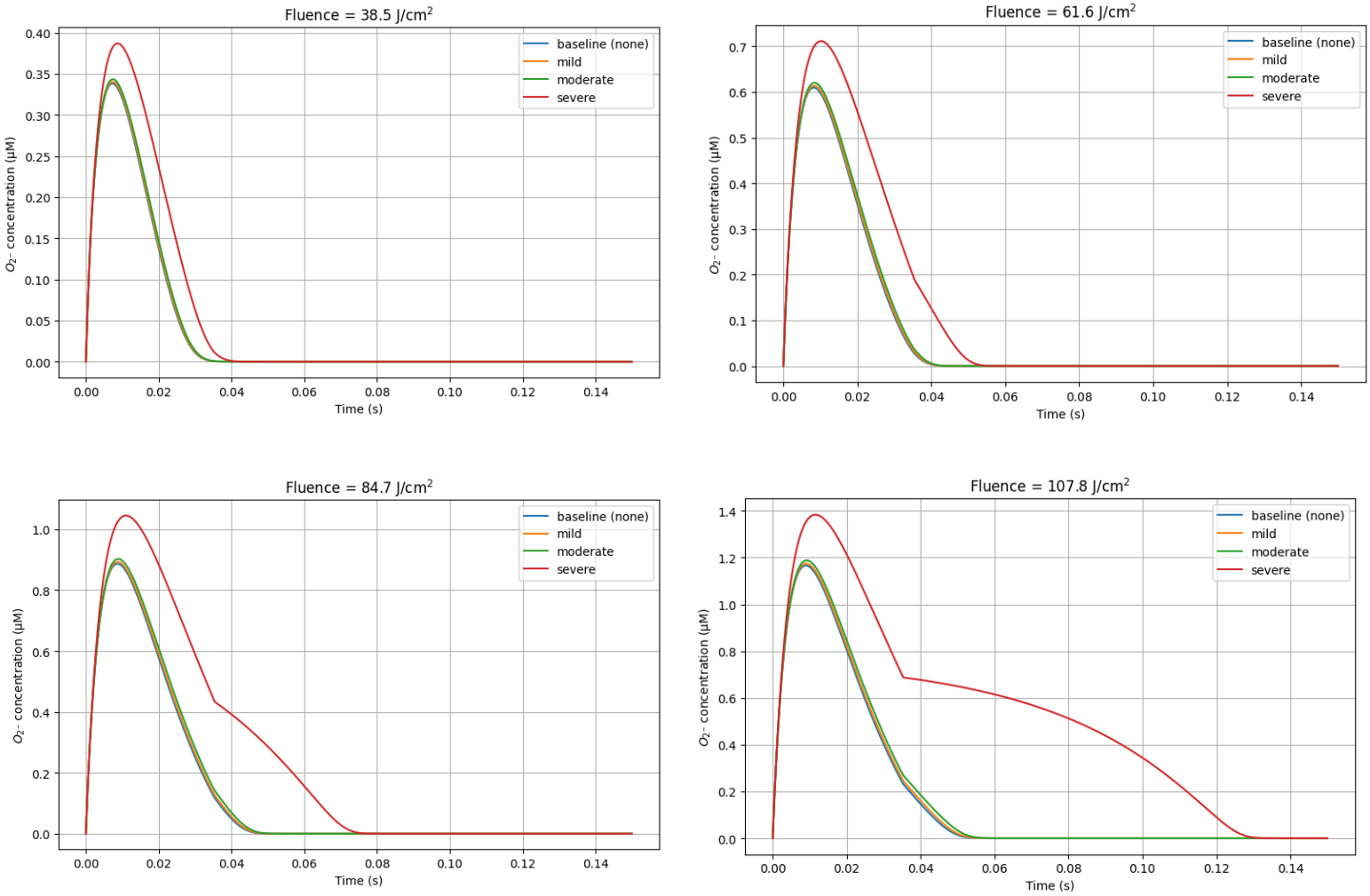

Figure 3 – Effect of Alcohol and PBM Light Fluence on Superoxide Concentration

The simulations above demonstrate that increased fluence levels during PBM lead to significant escalations in superoxide concentrations, particularly as acetaldehyde levels rise from baseline to moderate and severe categories. While changes in superoxide concentration at lower fluences (38.5 J/cm^2) are minimal, they become more pronounced at higher fluences (107.8 J/cm^2), with levels rising from approximately 0.32 μM to over 1 μM. This pattern indicates a prolonged oxidative stress response, delaying cellular recovery to steady state conditions and counteracting the benefits provided by PBM such as enhanced ATP synthesis. Therefore, accounting for alcohol consumption when recruiting patients is a key proactive measure in ensuring PBM efficacy.

4. Conclusion

PBM therapy takes advantage of natural cellular processes and uses light to induce therapeutic effects, offering a non-invasive alternative to conventional treatment for certain chronic conditions. However, just as alcohol is known to to adversely affect the efficacy of medications, it can similarly impair the benefits of PBM; even mild concentrations of alcohol have a minor effect in prolonging the decline in superoxide concentration back to steady state. This interaction highlights the growing need for ongoing research into ethanol's metabolic pathways and its role in regulating oxidative stress and ensuring ROS levels don't exist in excess quantities for extended periods of time. Overall, such mathematical models and insights are vital for developing targeted therapies that counteract the harmful effects of alcohol to ensure that each patient receives the most effective care while minimizing the impact of alcohol-related factors.

5. References

Aguirre, E., Rodríguez-Juárez, F., Bellelli, A., Gnaiger, E., & Cadenas, S. (2010). Kinetic model of the inhibition of respiration by endogenous nitric oxide in intact cells. Biochimica et Biophysica Acta (BBA) - Bioenergetics, 1797(5), 557–565. https://doi.org/10.1016/j.bbabio.2010.01.033

Amaroli, A., Pasquale, C., Zekiy, A., Utyuzh, A., Benedicenti, S., Signore, A., & Ravera, S. (2021). Photobiomodulation and oxidative stress: 980 nm diode laser light regulates mitochondrial activity and reactive oxygen species production. Oxidative Medicine and Cellular Longevity, 2021, 1–11. https://doi.org/10.1155/2021/6626286

Antunes, F., Boveris, A., & Cadenas, E. (2004). On the mechanism and biology of cytochrome oxidase inhibition by nitric oxide. Proceedings of the National Academy of Sciences, 101(48), 16774–16779. https://doi.org/10.1073/pnas.0405368101

Bathini, M., Raghushaker, C. R., & Mahato, K. K. (2020). The molecular mechanisms of action of photobiomodulation against Neurodegenerative Diseases: A systematic review. Cellular and Molecular Neurobiology, 42(4), 955–971. https://doi.org/10.1007/s10571-020-01016-9

Chung, H., Dai, T., Sharma, S. K., Huang, Y.-Y., Carroll, J. D., & Hamblin, M. R. (2011). The nuts and bolts of low-level laser (light) therapy. Annals of Biomedical Engineering, 40(2), 516–533. https://doi.org/10.1007/s10439-011-0454-7

Eriksson, C. J. P., Harada, S., Inoue, K., Jenkins, W. J., Julkunen, R. J. K., Lindros, K. O., Mizoi, Y., Pietruszko, R., Takase, S., Thomas, M., Tsutsumi, M., & Fukunaga, T. (2003, March 19). Changes in blood acetaldehyde levels after ethanol administration in alcoholics. Alcohol. https://www.sciencedirect.com/science/article/pii/074183299090058K?ref=pdf_download&fr=RR-2&rr=874e1eae9e473972

Fulop, A. M., Dhimmer, S., Deluca, J. R., Johanson, D. D., Lenz, R. V., Patel, K. B., Douris, P. C., & Enwemeka, C. S. (2010). A meta-analysis of the efficacy of laser phototherapy on pain relief. The Clinical Journal of Pain, 26(8), 729–736. https://doi.org/10.1097/ajp.0b013e3181f09713

Gendron, D. J., & Hamblin, M. R. (2019). Applications of photobiomodulation therapy to musculoskeletal disorders and osteoarthritis with particular relevance to Canada. Photobiomodulation, Photomedicine, and Laser Surgery, 37(7), 408–420. https://doi.org/10.1089/photob.2018.4597

Giulivi, C., Poderoso, J. J., & Boveris, A. (1998). Production of nitric oxide by mitochondria. Journal of Biological Chemistry, 273(18), 11038–11043. https://doi.org/10.1074/jbc.273.18.11038

Hamblin, M. R., & Demidova, T. N. (2006). Mechanisms of Low Level Light therapy. SPIE Proceedings. https://doi.org/10.1117/12.646294

Hoek, J. B., Cahill, A., & Pastorino, J. G. (2002). Alcohol and mitochondria: A dysfunctional relationship. Gastroenterology, 122(7), 2049–2063. https://doi.org/10.1053/gast.2002.33613

Hsieh, H.-C., Tseng, W.-W., & Wei, A.-C. (2022). Mathematical model of photobiomodulation on cytochrome c oxidase. 2022 IEEE 22nd International Conference on Bioinformatics and Bioengineering (BIBE). https://doi.org/10.1109/bibe55377.2022.00048

Jung, M. K., Callaci, J. J., Lauing, K. L., Otis, J. S., Radek, K. A., Jones, M. K., & Kovacs, E. J. (2010). Alcohol exposure and mechanisms of tissue injury and repair. Alcoholism: Clinical and Experimental Research, 35(3), 392–399. whThttps://doi.org/10.1111/j.1530-0277.2010.01356.x

Karu, T. I., Pyatibrat, L. V., & Afanasyeva, N. I. (2005). Cellular effects of low power laser therapy can be mediated by nitric oxide. Lasers in Surgery and Medicine, 36(4), 307–314. https://doi.org/10.1002/lsm.20148

Konstantinovic, L. M., Cutovic, M. R., Milovanovic, A. N., Jovic, S. J., Dragin, A. S., Letic, M. Dj., & Miler, V. M. (2010). Low-level laser therapy for acute neck pain with radiculopathy: A double-blind placebo-controlled randomized study. Pain Medicine, 11(8), 1169–1178. https://doi.org/10.1111/j.1526-4637.2010.00907.x

Lampl, Y., Zivin, J. A., Fisher, M., Lew, R., Welin, L., Dahlof, B., Borenstein, P., Andersson, B., Perez, J., Caparo, C., Ilic, S., & Oron, U. (2007). Infrared laser therapy for ischemic stroke: A new treatment strategy. Stroke, 38(6), 1843–1849. https://doi.org/10.1161/strokeaha.106.478230

Lucas, C., Criens-Poublon, L. J., Cockrell, C. T., & de Haan, R. J. (2002). Wound healing in cell studies and animal model experiments by low level laser therapy; were clinical studies justified? A systematic review. Lasers in Medical Science, 17(2), 110–134. https://doi.org/10.1007/s101030200018

Manzo-Avalos, S., & Saavedra-Molina, A. (2010). Cellular and mitochondrial effects of alcohol consumption. International Journal of Environmental Research and Public Health, 7(12), 4281–4304. https://doi.org/10.3390/ijerph7124281

Markevich, N. I., & Hoek, J. B. (2015). Computational modeling analysis of mitochondrial superoxide production under varying substrate conditions and upon inhibition of different segments of the electron transport chain. Biochimica et Biophysica Acta (BBA) - Bioenergetics, 1847(6–7), 656–679. https://doi.org/10.1016/j.bbabio.2015.04.005

Muggli, D. S., McCue, J. T., & Falconer, J. L. (1998). Mechanism of the photocatalytic oxidation of ethanol on tio2. Journal of Catalysis, 173(2), 470–483. https://doi.org/10.1006/jcat.1997.1946

Pastore, D., Martino, C. D., Bosco, G., & Passarella, S. (1996). Stimulation of ATP synthesis via oxidative phosphorylation in wheat mitochondria irradiated with helium-Neon Laser. IUBMB Life, 39(1), 149–157. https://doi.org/10.1080/15216549600201151

Peplow, P. V., Chung, T.-Y., & Baxter, G. D. (2009). Laser Photobiomodulation of wound healing: A review of experimental studies in mouse and rat animal models. Photomedicine and Laser Surgery, 28(3), 291–325. https://doi.org/10.1089/pho.2008.2446

Pryor, W. A., & Squadrito, G. L. (1995). The Chemistry of Peroxynitrite: A product from the reaction of nitric oxide with superoxide. American Journal of Physiology-Lung Cellular and Molecular Physiology, 268(5). https://doi.org/10.1152/ajplung.1995.268.5.l699

Roberts, B. J., Shoaf, S. E., Jeong, K. S., & Song, B. J. (1994). Induction of CYP2E1 in liver, kidney, brain and intestine during chronic ethanol administration and withdrawal: Evidence that CYP2E1 possesses a rapid phase half-life of 6 hours or less. Biochemical and Biophysical Research Communications, 205(2), 1064–1071. https://doi.org/10.1006/bbrc.1994.2774

Salehpour, F., Mahmoudi, J., Kamari, F., Sadigh-Eteghad, S., Rasta, S. H., & Hamblin, M. R. (2018). Brain Photobiomodulation therapy: A narrative review. Molecular Neurobiology, 55(8), 6601–6636. https://doi.org/10.1007/s12035-017-0852-4

Sfondrini, M. F., Vitale, M., Pinheiro, A. L., Gandini, P., Sorrentino, L., Iarussi, U. M., & Scribante, A. (2020). Photobiomodulation and pain reduction in patients requiring orthodontic band application: Randomized clinical trial. BioMed Research International, 2020, 1–10. https://doi.org/10.1155/2020/7460938

U.S. Department of Health and Human Services. (2023). Drinking levels defined. National Institute on Alcohol Abuse and Alcoholism (NIAAA). https://www.niaaa.nih.gov/alcohol-health/overview-alcohol-consumption/moderate-binge-drinking

Whelan, H. T., Smits, R. L., Buchman, E. V., Whelan, N. T., Turner, S. G., Margolis, D. A., Cevenini, V., Stinson, H., Ignatius, R., Martin, T., Cwiklinski, J., Philippi, A. F., Graf, W. R., Hodgson, B., Gould, L., Kane, M., Chen, G., & Caviness, J. (2001). Effect of NASA light-emitting diode irradiation on wound healing. Journal of Clinical Laser Medicine; Surgery, 19(6), 305–314. https://doi.org/10.1089/104454701753342758

Wong, H.-S., Dighe, P. A., Mezera, V., Monternier, P.-A., & Brand, M. D. (2017). Production of superoxide and hydrogen peroxide from specific mitochondrial sites under different bioenergetic conditions. Journal of Biological Chemistry, 292(41), 16804–16809. https://doi.org/10.1074/jbc.r117.789271

Wong-Riley, M. T. T., Liang, H. L., Eells, J. T., Chance, B., Henry, M. M., Buchmann, E., Kane, M., & Whelan, H. T. (2005). Photobiomodulation directly benefits primary neurons functionally inactivated by toxins. Journal of Biological Chemistry, 280(6), 4761–4771. https://doi.org/10.1074/jbc.m409650200

Xavier, M., David, D. R., de Souza, R. A., Arrieiro, A. N., Miranda, H., Santana, E. T., Silva, J. A., Salgado, M. A., Aimbire, F., & Albertini, R. (2010). Anti-inflammatory effects of low-level light emitting diode therapy on achilles tendinitis in rats. Lasers in Surgery and Medicine, 42(6), 553–558. https://doi.org/10.1002/lsm.20896

6. Appendix

AMATH 382 Final Project Graphs